Journal of Computational Neuroscience 17, 245–261, 2004

The Activity Phase of Postsynaptic Neurons in a Simplified Rhythmic Network

AMITABHA BOSE
Department of Mathematical Sciences, New Jersey Institute of Technology, Newark, NJ 07102, USA
bose@njit.edu

YAIR MANOR
Life Sciences Department, Ben-Gurion University of the Negev and Zlotowski Center for Neuroscience, Beer-Sheva, Israel 84105
yairman@bgumail.bgu.ac.il

FARZAN NADIM
Department of Mathematical Sciences, New Jersey Institute of Technology, Newark, NJ 07102, USA; Department of Biological Sciences, Rutgers University, Newark, NJ 07102, USA
farzan@njit.edu

Received April 27, 2004; Revised June 9, 2004; Accepted June 14, 2004

Action Editor: David Terman

Abstract. Many inhibitory rhythmic networks produce activity in a range of frequencies. The relative phase of activity between neurons in these networks is often a determinant of the network output. This relative phase is determined by the interaction between synaptic inputs to the neurons and their intrinsic properties. We show, in a simplified network consisting of an oscillator inhibiting a follower neuron, how the interaction between synaptic depression and a transient potassium current in the follower neuron determines the activity phase of this neuron. We derive a mathematical expression to determine at what phase of the oscillation the follower neuron becomes active. This expression can be used to understand which parameters determine the phase of activity of the follower as the frequency of the oscillator is changed. We show that in the presence of synaptic depression, there can be three distinct frequency intervals, in which the phase of the follower neuron is determined by different sets of parameters. Alternatively, when the synapse is not depressing, only one set of parameters determines the phase of activity at all frequencies.

Keywords: A-current, synaptic depression, phase maintenance, central pattern generator

1. Introduction

Many behaviors result from rhythmic activity of neuronal networks in which different groups of neurons are active at different times during the rhythm cycle. In most cases, such rhythms operate in a wide range of frequencies (Marder and Calabrese, 1996). In order for the network to produce a meaningful output, there needs to be a coordination between the activity patterns of these groups. For example, irrespective of frequency, different neurons may fire with a fixed latency, or a fixed phase, with respect to each other (Ahissar et al.,

2000; Bartos et al., 1999). In other cases, the timing of activity may be a combination of these two relationships (Hooper, 1997a, b; Pearson and Iles, 1970).

Typically one might expect a fixed latency between the firing of the pre- and the postsynaptic neuron, independent of the activation frequency of the synapse (DiCaprio et al., 1997). It is less clear how two neurons could have a prescribed phase difference, independent of frequency, because the mechanism responsible for this temporal relationship would need continuous access to the rhythm frequency. Such a mechanism, if it exists, could be either externally imposed on, or emerge as a built-in property of the network. A recent computational study proposed that the dynamics of a synapse could be used to automatically set the phase between two neurons (Manor et al., 2003). This study demonstrated that a depressing inhibitory synapse between an oscillator and a follower neuron could produce a fixed phase difference between the two neurons across a relatively wide range of frequencies.

The mechanism proposed by Manor et al. (2003) depended only upon the dynamics of the synapse and did not take account of other built-in elements such as intrinsic properties of the follower neuron. However, as demonstrated in previous studies, intrinsic currents, such as the transient potassium (A) current, may also be involved in delaying or advancing the onset of activity in follower neurons (Harris-Warrick et al., 1995). The A current plays a very important role in determining the relationship between spike frequency and injected current in neurons (Connor and Stevens, 1971). In particular, the distinction between Type I and Type II neurons was originally shown by adding an A current to the Hodgkin-Huxley equations (Connor et al., 1977). The A current also plays a significant role in determining the activity of a neuron on rebound from synaptic inhibition (Harris-Warrick et al., 1995; Hess and Manira, 2001; Hsiao and Chandler, 1995). The effect of this ionic current in shaping the activity of neurons has been the subject of several modeling studies (Buchholtz et al., 1992; Rush and Rinzel, 1995).

In this work we study how synaptic and intrinsic dynamics interact to determine phase in a simple oscillator-follower network. In particular, we investigate the interplay between a depressing inhibitory synapse and the A current in the follower neuron. We choose to focus on the A current because it produces a post-inhibitory delay in the activity of the follower neuron. The A current is, of course, only one of several intrinsic currents that may contribute to the activity phase of the follower neuron. The analysis and insights of this work can be applied to understand the contribution of other types of currents, such as the hyperpolarization-activated inward current or a low-threshold calcium current.

The model we study consists of a simplified network in which the presynaptic neuron is simply a square-wave oscillator and the follower is a generic two-variable excitable neuron, modified by adding an A current. The small number of variables in this model enables us to use phase-plane analysis to derive a mathematical expression for the phase difference between the oscillator and the follower neuron. The mathematical techniques provide a novel way to incorporate the effects of the A current in a phase plane model. Moreover, this analytical approach allows us to pinpoint the parameters that most significantly affect phase in different frequency domains.

We find that, with a non-depressing synapse, there is a fixed latency between the activity of the oscillator and the follower neuron, independent of frequency. In contrast, with the appropriate choice of parameters, a depressing synapse causes the latency to increase as the oscillation frequency is decreased. Moreover, as this latency becomes longer, the size of the A current in the follower neuron increases, in turn, increasing the latency even further. Thus, synaptic depression acts synergistically with the A current to control the activity phase of the follower neuron. In particular, we find that there can be three separate frequency intervals in which the phase of the follower neuron is determined by different and independent parameters. Thus, intrinsic properties in conjunction with synaptic dynamics can considerably extend the frequency range for which phase may be controlled.

2. Model and Equations

2.1. The Oscillator Neuron O

In this study we focus only on the effect of an oscillator neuron O inhibiting a follower neuron F. For simplicity, the activity of O is described by a periodic square wave pulse with voltage v_O. We denote the length of the active state of O ($v_O > v_{\text{thresh}}$) by T_{act}, and the length of the inactive state ($v_O < v_{\text{thresh}}$) by T_{inact}, where v_{thresh} denotes the threshold for synaptic transmission. The period of O is given by $P = T_{\text{act}} + T_{\text{inact}}$.

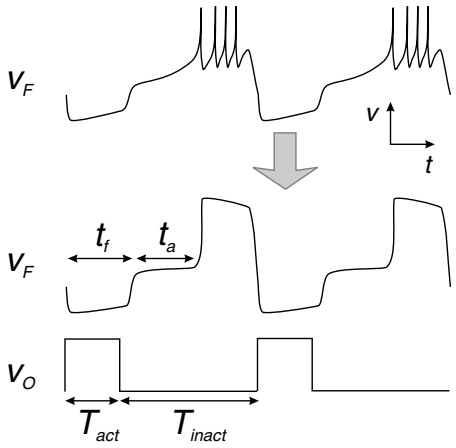

Figure 1. Approximation of the biological voltage trace. The top voltage trace shows an experimental recording from a crab pyloric PY neuron in response to periodic injection of negative current. We approximate this trace by the smooth middle trace. The bottom trace shows a square wave pulse, representing the oscillator. Important time lengths and timing relationships are also indicated.

2.2. *Intrinsic Dynamics of the Follower Neuron F*

The top trace of Fig. 1 shows a typical intracellular voltage trace of a follower PY neuron recorded from the crab pyloric nervous system entrained to follow a periodic stimulus (Nadim, unpublished data). The trace can be divided into three parts: spikes riding on top of a burst envelope, a low-voltage hyperpolarized state and an intermediate-voltage state leading up to the spiking activity. The periodic activity of the PY neuron *in vivo* results from synaptic inhibition that it receives from the pacemaker neurons of the pyloric network. In the trace shown in Fig. 1, this neuron is synaptically isolated and the input from the pacemaker neurons is replaced by a periodically injected negative current pulse. This PY neuron is a biological representative of the follower neuron F in this study. Our results focus on the (bursting) activity of the follower neuron while ignoring the exact timing of the individual spikes. As such, we shall approximate the activity of a bursting neuron with a voltage trace that smooths over the spikes (middle trace of Fig. 1). We shall keep track of two important time intervals related to the activity of F. The first is t_f; it is the time that the follower neuron F stays in the low-voltage silent state. The second is t_a; it is the time that the follower neuron F stays in the intermediate-voltage state. The main goal of this work is to derive analytical expressions for t_f, t_a and phase ($\phi = [t_f + t_a]/P$) as a function of the period P of the oscillator O.

The activity of the follower neuron F is governed by biophysical current balance equations. We begin with a simple 2-dimensional excitable neuronal model (such as a Morris-Lecar or Fitzhugh-Nagumo type neuron) that does not yet incorporate the A current. The activity of such a neuron can be geometrically represented in a 2-dimensional phase plane with equations that produce a cubic shaped voltage nullcline (Rinzel and Ermentrout, 1997). We will not be concerned with the exact form of these equations, only with their qualitative dynamics. Thus, we present them in general form:

$$\begin{aligned} \epsilon v' &= f(v, w) \\ w' &= [w_\infty(v) - w]/\tau_w(v), \end{aligned} \tag{1}$$

where v represents the voltage of F, w is the recovery variable and the derivative is with respect to time t. The v-nullcline $\mathcal{C}_o = \{(v, w) : f(v, w) = 0\}$ is a cubic shaped curve, while the w-nullcline $\mathcal{S}_o = \{(v, w) : w_\infty - w = 0\}$ is a sigmoidal shaped curve (Fig. 2A). The function $f(v, w)$ is positive (negative)

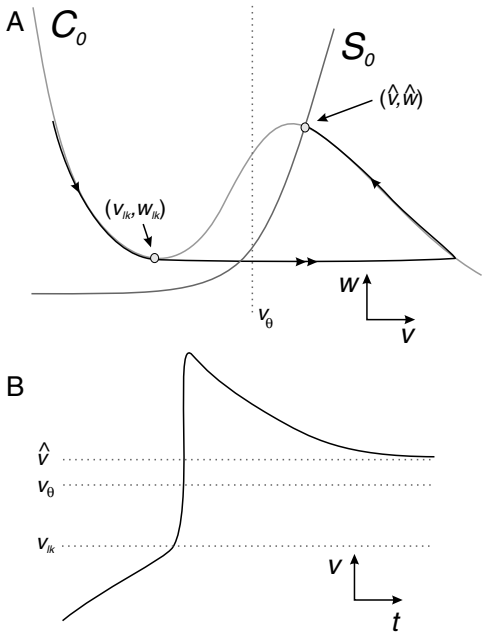

Figure 2. (A) The $v - w$ phase plane. The v-nullcline $\mathcal{C}_o$ and the w-nullcline $\mathcal{S}_o$ intersect uniquely at $(\hat{v}, \hat{w})$. A portion of the trajectory is superimposed on the phase plane. It consists of three main parts: slow evolution along the left and right branches of $\mathcal{C}_o$ and fast evolution between these branches. The transition from the right to left branch is not shown. (B) The corresponding voltage trace of F is shown. Also marked, with dotted lines, are the values of v_{lk}, v_θ and $\hat{v}$.

below (above) $\mathcal{C}_o$. We shall assume that $\mathcal{C}_o$ and $\mathcal{S}_o$ intersect at only one point $(\hat{v}, \hat{w})$ where $\hat{w} = w_\infty(\hat{v})$ along the right branch of $\mathcal{C}_o$, ensuring that the isolated F neuron has a stable, high voltage steady state. We denote the local minimum of $\mathcal{C}_o$ by (v_{lk}, w_{lk}).

When ϵ is small enough, Eq. (1) involves two distinct time scales (i.e., the system is singularly perturbed). These time scales control the trajectory of F in different regions of the phase space. The F trajectory can be divided into regions with slow movements at low- or high-voltage states and fast transitions between these states (Fig. 2). We will employ geometric singular perturbation theory to track the trajectory of F in the $v-w$ phase plane (Mishchenko and Rozov, 1980). This involves deriving reduced (lower dimensional) sets of equations which govern the evolution of F along different parts of its trajectory. By setting $\epsilon = 0$ in Eq. (1), we obtain the slow equations

$$\begin{aligned} 0 &= f(v, w) \\ w' &= [w_\infty(v) - w]/\tau_w(v). \end{aligned} \tag{2}$$

The first equation forces F to lie on the $\mathcal{C}_o$ nullcline. The second equation governs the evolution of w (and in turn v) along $\mathcal{C}_o$. In particular, when F lies on the left branch of $\mathcal{C}_o$, then $w' < 0$ and on the right branch $w' > 0$. By rescaling time $t = \epsilon\xi$ and then setting $\epsilon = 0$, we obtain the fast equations (derivative below is with respect to ξ).

$$\begin{aligned} \dot{v} &= f(v, w) \\ \dot{w} &= 0 \end{aligned} \tag{3}$$

These equations govern fast transitions (or jumps) between the left and right branches of $\mathcal{C}_o$. A fast transition is a heteroclinic solution (connecting two critical points) of Eq. (3). For example, it may connect (v_{lk}, w_{lk}) on the left branch of $\mathcal{C}_o$ to a point (v_r, w_{lk}) on the right branch of $\mathcal{C}_o$. The jumps between the silent and active states of F occur instantaneously with respect to the slow time t (Fig. 2). Figure 2B shows the voltage trace of F corresponding to the trajectory shown in Fig. 2A. A neuron will said to be active if $v > v_\theta$ (the trajectory of F lies on the right branch of $\mathcal{C}_o$) and silent if $v < v_\theta$ (the trajectory of F lies on the left branch of $\mathcal{C}_o$), where v_θ satisfies $v_{lk} < v_\theta < \hat{v}$.

For simplicity of the analysis, we assume that w_∞ is 0 for v values on the left branch of $\mathcal{C}_o$. We will also assume that the time constant $\tau_w(v)$ of the recovery variable w assumes, respectively, the values τ_L and τ_R on the left and right branches of $\mathcal{C}_o$. These values determine the rate of evolution of F in its silent and active states (Fig. 2).

2.3. *The A Current*

The A current is modeled by $I_A = \bar{g}_a a_m a_h [v - E_K]$, where a_m and a_h respectively govern the activation and inactivation kinetics. The parameters $\bar{g}_a$ and E_K are the maximal conductance and reversal potential of the A current. The inactivation variable a_h obeys the first order kinetic equation

$$a_h' = [h_\infty(v) - a_h]/\tau_h(v), \tag{4}$$

where $h_\infty(v) = 1/[1 + \exp((v - v_m)/k_h)]$. The parameter v_m should satisfy $v_{lk} < v_m \leq v_\theta$ so that the A current recovers from inactivation on the left branch of the v-nullcline and starts to inactivate as soon as the F trajectory leaves the left branch. For simplicity of calculations we make a few assumptions. First, we assume that $k_h \to 0$, which will make the curve h_∞ a step function equal to 1 for v below v_m and 0 otherwise. Second, we also assume instantaneous all-or-none activation kinetics $a_m = a_m(v) = H(v - v_\theta)$ where H is the Heaviside function. I_A recovers from inactivation when the F trajectory is on the left branch of the v-nullcline and inactivates otherwise. We will also assume that $\tau_h(v)$ is equal to τ_{lo} on the left branch of $\mathcal{C}_o$, τ_{hi} on the right branch of $\mathcal{C}_o$ and τ_{med} in a neighborhood of $v = v_\theta$. We assume that τ_{hi} is sufficiently small so that a_h quickly decays toward 0 when v is large. With this assumption, there is no residual A current affecting the behavior of F when O becomes active again, making the calculations somewhat simpler.

The equations that govern the activity of F can now be written as

$$\begin{aligned} \epsilon v' &= f(v, w) - \bar{g}_a a_m a_h [v - E_K] \\ w' &= [w_\infty(v) - w]/\tau_w(v) \\ a_h' &= [h_\infty(v) - a_h]/\tau_h(v) \\ a_m &= H(v - v_\theta). \end{aligned} \tag{5}$$

We now define reduced equations which govern the evolution of F in different parts of its trajectory. When F is in the silent state, $a_m(v) = 0$. Thus the slow equations governing the activity of F in the silent state are

$$\begin{aligned} 0 &= f(v, w) \\ w' &= -w/\tau_L \\ a_h' &= [1 - a_h]/\tau_{\text{lo}}. \end{aligned} \tag{6}$$

Note that while an equation for a_h is included in (6), a_h does not actually affect F in the silent state because $a_m = 0$. However, upon leaving the silent state, the value of a_h affects the F dynamics. When F is in the active state, $a_m(v) = 1$ and the slow equations are

$$\begin{aligned} 0 &= f(v, w) - \bar{g}_a a_h [v - E_K] \\ w' &= [w_\infty(v) - w]/\tau_R \\ a_h' &= -a_h/\tau_{\text{hi}}. \end{aligned} \tag{7}$$

There are two sets of fast equations which govern the transition of F from the silent to the active state. On the interval $v_{lk} < v < v_\theta$ the fast equations are

$$\begin{aligned} \dot{v} &= f(v, w) \\ \dot{w} &= 0 \\ \dot{a}_h &= 0, \end{aligned} \tag{8}$$

whereas for $v_\theta < v$ these equations are

$$\begin{aligned} \dot{v} &= f(v, w) - \bar{g}_a a_h [v - E_K] \\ \dot{w} &= 0 \\ \dot{a}_h &= 0. \end{aligned} \tag{9}$$

As we will show in the Results section, the addition of an A current in (9) causes the v-nullcline of F to have a quintic shape. We refer to this quintic v-nullcline as $\mathcal{Q}_o$. The simplifying assumption that the activation of the A current is all-or-none restricts this middle branch of $\mathcal{Q}_o$ to lie on $v = v_\theta$. For simplicity of analysis, we will assume that the kinetics of the intrinsic variable w on the middle branch are much slower than the inactivation of the A current (in a neighborhood of v_θ, $\tau_w(v) \gg \tau_{\text{med}}$). Thus on the middle branch, w does not change and remains at the value w_{lk} from which the F trajectory left the silent state. With this assumption, the equations for F on the middle branch are

$$\begin{aligned} v' &= 0 \\ w' &= 0 \\ a_h' &= -a_h/\tau_{\text{med}}. \end{aligned} \tag{10}$$

2.4. The O to F Synapse

The synapse from O to F is modeled as an inhibitory depressing synapse (Bose et al., 2001; Manor et al., 2003). The synaptic current is incorporated in the model by adding the term $I_{\text{syn}} = \bar{g}_{\text{syn}} s[v - E_{\text{syn}}]$ to the right side of the v equations in Eqs. (5)–(9). The parameters $\bar{g}_{\text{syn}}$ and E_{syn} are the maximal conductance and reversal potential of the synapse, respectively. To ensure that the synapse is inhibitory, we choose E_{syn} to be less than v_{lk}. The variable s denotes the synaptic efficacy and lies between 0 and 1. The value of s depends on another variable d that measures the extent of depression in the inhibitory synapse. The equations governing s and d are

$$\begin{aligned} d' &= \begin{cases} (1-d)/\tau_\alpha & v_O < v_{\text{thresh}} \\ -d/\tau_\beta & v_O \geq v_{\text{thresh}} \end{cases} \\ s' &= \begin{cases} -s/\tau_\kappa & v_O < v_{\text{thresh}} \\ (d_0 - s)/(\epsilon\tau_\eta) & v_O \geq v_{\text{thresh}} \end{cases} \end{aligned} \tag{11}$$

where d_0 is the value of d when O becomes active (v_O crosses v_{thresh} with positive slope). Figure 3 shows time traces of variables d and s for two cycles of the oscillator neuron O. When O becomes active, s approaches d_0 with time constant $\epsilon\tau_\eta$. In the limit as $\epsilon \to 0$ this implies that $s = d_0$ during the entire active state of O. When O becomes silent, s decays with time constant τ_κ. The parameters τ_α and τ_β are the recovery and depression time constants, respectively. These time constants determine the dependence of d on the activity of the oscillator O (Fig. 3).

The value d_0 can be calculated using the periodicity of O. From Eq. (11), when O becomes active, $d' = -d/\tau_\beta$. Thus $d(T_{\text{act}}) = d_0 \exp(-T_{\text{act}}/\tau_\beta)$. When O is silent $d' = [1-d]/\tau_\alpha$. Solving this equation with the condition on $d(T_{\text{act}})$ given above and using the periodicity condition $d(T_{\text{act}} + T_{\text{inact}}) = d_0$, we obtain

$$d_0 = \frac{1 - \exp(-T_{\text{inact}}/\tau_\alpha)}{1 - \exp(-T_{\text{inact}}/\tau_\alpha)\exp(-T_{\text{act}}/\tau_\beta)}.$$

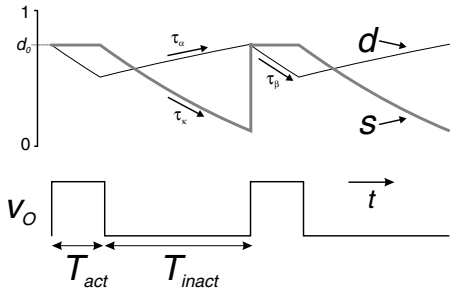

Figure 3. Dynamics of the synaptic (s) and the depression (d) variables are shown. In the lower trace, the voltage of the oscillator is shown. When the oscillator is active, d depresses with time constant τ_β while s is constant. When the oscillator is active, d recovers with time constant τ_α, while s decays with time constant τ_κ. The variable s is reset to d whenever O becomes active.

For convenience we keep track of the synaptic conductance $g_s = \bar{g}_{\text{syn}} s$ instead of the synaptic variable s. Just before O becomes active, g_s is at its minimum value denoted by $g_{\min}$. Just after it becomes active, g_s is reset to its maximum value denoted by g_{peak} (see the s trace in Fig. 3). The value $g_{\text{peak}} = \bar{g}_{\text{syn}} d_0$, which can be rewritten as

$$g_{\text{peak}} = \bar{g}_{\text{syn}} \frac{1 - \exp(-T_{\text{inact}}/\tau_\alpha)}{1 - \exp(-T_{\text{inact}}/\tau_\alpha)\exp(-T_{\text{act}}/\tau_\beta)}. \tag{12}$$

The above equation shows how the relative strength of the depressing synapse depends on the time constants of recovery and depression, and on T_{act} and T_{inact}. Thus in the case where the synapse is depressing, as period changes, g_{peak} will, in general, change as well. However when we consider cases involving a non-depressing synapse, we let $d(t) \equiv 1$ and thus g_{peak} is constant.

2.5. *The Reduced Equations*

The activity of F in the presence of synaptic input from O and an intrinsic A current is governed by

$$\begin{aligned}
\epsilon v' &= f(v, w) - \bar{g}_a a_h a_m [v - E_K] - g_s [v - E_{\text{syn}}] \\
w' &= [w_\infty(v) - w]/\tau_w(v) \\
a_h' &= [h_\infty(v) - a_h]/\tau_h(v) \\
a_m &= H(v - v_\theta) \\
d' &= \begin{cases} (1-d)/\tau_\alpha & v_O < v_{\text{thresh}} \\ -d/\tau_\beta & v_O \geq v_{\text{thresh}} \end{cases} \\
g_s' &= \begin{cases} -g_s/\tau_\kappa & v_O < v_{\text{thresh}} \\ (\bar{g}_{\text{syn}} d_0 - g_s)/(\epsilon \tau_\eta) & v_O \geq v_{\text{thresh}}. \end{cases}
\end{aligned} \tag{13}$$

The activity of F on different branches of the quintic v-nullcline is governed by reduced equations obtained when setting $\epsilon = 0$ in Eq. (13). These are the equations upon which all the analyses in this work are based. When O is active (and F is silent) then

$$\begin{aligned}
0 &= f(v, w) - g_s [v - E_{\text{syn}}] \\
w' &= -w/\tau_L \\
a_h' &= [1 - a_h]/\tau_{\text{lo}} \\
d' &= -d/\tau_\beta \\
g_s &= g_{\text{peak}},
\end{aligned} \tag{14}$$

where g_{peak} is given by Eq. (12). When O and F are both silent then

$$\begin{aligned}
0 &= f(v, w) - g_s [v - E_{\text{syn}}] \\
w' &= -w/\tau_L \\
a_h' &= [1 - a_h]/\tau_{\text{lo}} \\
d' &= [1 - d]/\tau_\alpha \\
g_s' &= -g_s/\tau_\kappa.
\end{aligned} \tag{15}$$

When O is silent and F is on the middle branch of the quintic v-nullcline then

$$\begin{aligned}
v' &= 0 \\
w' &= 0 \\
a_h' &= -a_h/\tau_{\text{med}} \\
d' &= [1 - d]/\tau_\alpha \\
g_s' &= -g_s/\tau_\kappa.
\end{aligned} \tag{16}$$

Finally, when O is silent and F is active then

$$\begin{aligned}
0 &= f(v, w) - g_s [v - E_{\text{syn}}] - \bar{g}_a a_h [v - E_K] \\
w' &= [w_\infty(v) - w]/\tau_R \\
a_h' &= -a_h/\tau_{\text{hi}} \\
d' &= [1 - d]/\tau_\alpha \\
g_s' &= -g_s/\tau_\kappa.
\end{aligned} \tag{17}$$

3. Results

Our general goal is to derive a mathematical expression for the activity phase ϕ of the follower neuron F in terms of parameters of the depressing synapse and the A current. The results are divided into three main parts. In the first part, we derive an expression for t_f (Fig. 1), the time that F spends in its inhibited or silent state (on the left branch of its v nullcline). In Section 3.1 we show the effect of synaptic inhibition on the F nullclines. We then describe how depression determines the peak of the synaptic strength at different periods of O. In Section 3.2, we derive Eq. (18) that describes how t_f is related to the parameters of the model.

The contribution of the A current is dealt with in the second part of the results. Here, we derive an expression for t_a (Fig. 1), the time delay produced by the A current between the silent (low-voltage) and active (high-voltage) states of F. This is done by first

establishing the effect of the A current on the F nullclines in Section 3.3. In this section we also provide a necessary condition, Eq. (22), for the A current to produce a delay (i.e., $t_a > 0$). In Section 3.4 we use these conditions to derive an estimate (Eq. (25)) on how large t_f needs to be in order for $t_a > 0$. Assuming Eq. (25) is satisfied, we then derive an Eq. (27) that describes how t_a is related to t_f and other parameters of the model.

Finally, in Section 3.5, the expressions for t_f and t_a are used to compute the phase ϕ of F activity. We examine the dependence of phase on period P for one specific case where the period is changed by changing only the duration of the silent state of the oscillator (T_{inact}). In this section we demonstrate the phase versus period relationships for four cases: no depression and no A current, no depression with A current, depression and no A current, and depression with A current.

3.1. *The Effect of the O to F Synapse on the Nullclines of F*

Inhibition, in general, tends to shift the v nullcline $\mathcal{C}_o$ down in the $v - w$ phase plane and the greater the inhibition (larger g_{peak}), the larger the shift in $\mathcal{C}_o$ (Fig. 4). Inhibition causes the F trajectory to land on the left branch, as shown in panels A and B of Fig. 4. If synaptic inhibition (g_s) does not decay while O is silent, the trajectory of F would remain on the cubic nullcline corresponding to $g_s = g_{\text{peak}}$ (the lower nullcline of panels A and B). However, since the strength of inhibition decays with time constant τ_κ when O is silent, the trajectory of F does not stay on any one cubic nullcline; it starts from the nullcline corresponding to $g_s = g_{\text{peak}}$ and moves towards the nullcline $\mathcal{C}_o$ corresponding to $g_s = 0$. This can be seen in the trajectories shown in panels A and B.

The local minimum points of these inhibited cubics form a curve (Fig. 4A and B). The trajectory of F must reach this curve in order for F to leave the silent state. We call this curve the jump curve. Note that when the inhibition is weak, the jump curve does not intersect the sigmoidal nullcline $\mathcal{S}_o$ (Fig. 4A). However, when the inhibition is strong, the jump curve and $\mathcal{S}_o$ intersect (Fig. 4B). The value of g_s at which the jump curve intersects $\mathcal{S}_o$ is denoted g_s^*.

Inhibition also shifts down the right branches of the cubic nullcline (Fig. 4C). Thus, once O becomes active again, it causes F to jump down to the left branch of the cubic with $g_s = g_{\text{peak}}$ and $w = w_0$ which is smaller than but close to $\hat{w}$.

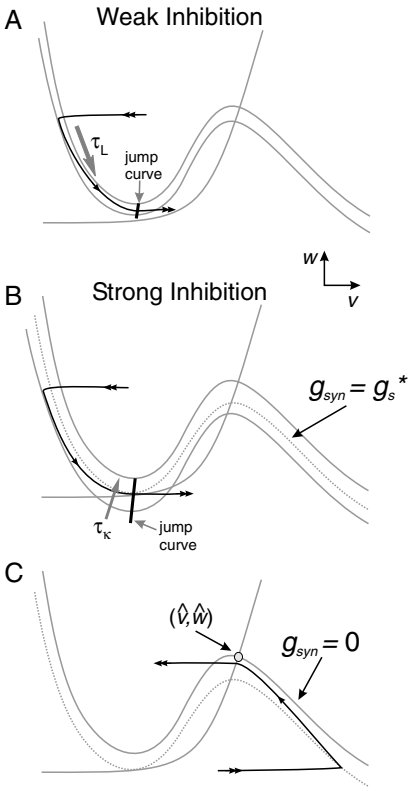

Figure 4. Effect of inhibition on the v-nullcline. In panels A and B, the local minima of the cubics forms a curve, called the jump curve. (A) When inhibition is weak, the time constant of w (τ_L) is the primary determinant of how much time t_f F spends in the silent state before reaching the jump curve. (B) When inhibition is strong, the time constant of decay of the synapse (τ_κ) primarily determines this time. The dashed cubic corresponds to $g_s = g_s^*$ at which the cubic is tangent to $\mathcal{S}_o$ on the left branches C. The trajectory of F never reaches the fixed point $(\hat{v}, \hat{w})$, but leaves the right branches due to inhibition while near this fixed point.

When the synapse is depressing, the strength of inhibition is a function of the period of O as determined by Eq. (12). Thus, depending on the period of O, the inhibitory synapse may be weak, resulting in an F trajectory as in Fig. 4A, or strong, resulting in an F trajectory as in Fig. 4B.

3.2. *The Dependence of t_f on the Oscillation Period and the Synaptic and Intrinsic Parameters*

In this section we derive the time delay t_f between the onset of activity in O and the onset of activity in F when F does not have an A current ($\bar{g}_a = 0$). This is the time that F spends on the left branch of the v-nullcline.

Let's assume that F jumps to the left branch at $t = 0$. In order to calculate t_f we follow the trajectory of F on the left branch of $\mathcal{C}_o$ (see Fig. 4). The part of the trajectory is controlled by the dynamics of two independent variables g_s and w. This trajectory ends at the "jump curve", the curve where the left branch of the v nullcline loses stability in the fast system. The jump curve can be linearly approximated as $g_s = g_s^* - Mw$ where the parameter M is a positive constant (Bose et al., 2001). The parameter M is a proportionality factor that indicates that a jump point with a smaller value of w corresponds to stronger inhibition (larger g_s; see Fig. 4A and B).

At the time ($t = 0$) when O becomes active and F jumps to the silent state, $g_s(0) = g_{\text{peak}}$ and $w(0) = w_0$. Thus, using this linear relationship for the jump curve and the reduced Eqs. (14) and (15) we obtain the following implicit equation involving t_f:

$$g_{\text{peak}} \exp(-(t_f - T_{\text{act}})^+/\tau_\kappa) + Mw_0 \exp(-t_f/\tau_L) = g_s^*, \tag{18}$$

where $(t_f - T_{\text{act}})^+ = t_f - T_{\text{act}}$ if $t_f > T_{\text{act}}$ or 0 if $t_f < T_{\text{act}}$. Equation (12) for g_{peak} and Eq. (18) completely determine the delay t_f. In the case of a non-depressing synapse, g_{peak} is constant for all values of P. Thus, Eq. (18) implies that t_f is constant for all P. In contrast, when the synapse is depressing t_f may be dependent on P since g_{peak} is a function of T_{inact} and T_{act}.

When g_{peak} is either large enough or small enough, Eq. (18) can be simplified and explicitly solved for t_f. When g_{peak} is small enough ($g_{\text{peak}} \ll Mw_0$), the first term on the left hand side of Eq. (18) can be ignored and the equation can be solved for t_f to obtain

$$t_f = \tau_L \ln \frac{Mw_0}{g_s^*}. \tag{19}$$

The time t_f in this case is constant with respect to P and mainly determined by τ_L which is an intrinsic time constant of F governing its evolution in the silent state (Fig. 4A). In contrast, when g_{peak} is large, the first term on the left hand side Eq. (18) can dominate the second. This will occur if $\bar{g}_{\text{syn}} > g_s^*$ and $\tau_\kappa \gg \tau_L$. Again the equation can be solved for t_f to obtain

$$t_f = \tau_\kappa \ln \frac{g_{\text{peak}}}{g_s^*} + T_{\text{act}}. \tag{20}$$

Here the most relevant time constant in determining t_f is τ_κ, the time constant of synaptic decay following the active state of O. In this case (large g_{peak}), t_f is an increasing function of g_{peak}.

3.3. *The Effect of the A Current on the Nullclines*

Now that we have established the dependence of t_f on P in the presence of depression, we will describe how the existence of an outward A current in the follower neuron F can affect this relationship. We shall do this in two steps. First, we will establish the conditions that must hold for the A current to produce a delay in the activity of F. This additional delay would occur in the transition of F from the silent state (the left branch of the v nullcline) to the active state (the right branch of the v nullcline). Second, we will measure the additional delay caused by the A current once these conditions are satisfied.

We will first discuss the effect of the A current on the dynamics of F in the absence of the inhibitory synapse. The effect of the A current is to change the shape of the v nullcline. Specifically, the additional term $\bar{g}_a a_h[v - E_K]$ in Eq. (9) causes the part of $\mathcal{C}_o$ to the right of $v = v_\theta$ (where the A current activates) to shift down in the phase plane. The larger the magnitude of I_A, the larger the shift (Fig. 5). Thus the v-nullcline in the presence of I_A, as given by Eqs. (8) and (9) is quintic shaped. We denote this quintic nullcline as $\mathcal{Q}_o$. The middle branch of $\mathcal{Q}_o$ lies on the vertical line $v = v_\theta$. The local maximum along the middle branch of $\mathcal{Q}_o$ occurs at $w = w_\theta$ where w_θ satisfies $f(v_\theta, w_\theta) = 0$. The minimum value depends on how big a_h becomes while

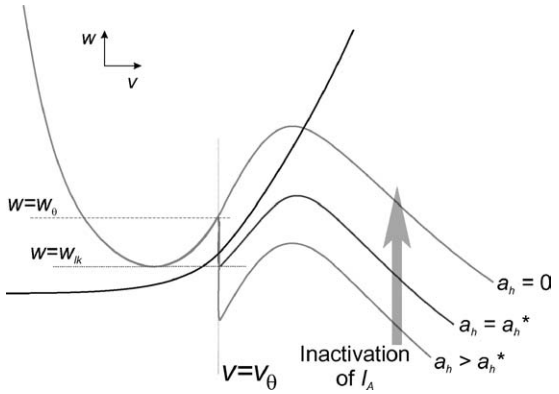

Figure 5. The frequency-dependent effect of the A current on the v-nullcline. The A current only affects the v-nullcline when $v \geq v_\theta$. The middle branch of any quintic shaped nullcline lies on $v = v_\theta$. The one with $a_h = a_h^*$ has $w = w_{lk}$ as its minimum value. The right side of the nullclines moves up as a_h decreases.

F is in the silent state. Since F leaves the silent state when $t = t_f$, the size of the A current at this instant is determined by $a_h(t_f) = [1 - \exp(-t_f/\tau_{\text{lo}})]$. Therefore the minimum w value along the middle branch, denoted $w_{\min}$, satisfies

$$f(v_\theta, w_{\min}) - \bar{g}_a a_h(t_f)[v_\theta - E_K] = 0.$$

In the absence of synaptic input, F leaves the silent state from w_{lk}. Let us denote by a_h^* the value of a_h which satisfies

$$f(v_\theta, w_{lk}) - \bar{g}_a a_h^*[v_\theta - E_K] = 0.$$

By solving for a_h^*, we obtain

$$a_h^* = \frac{f(v_\theta, w_{lk})}{\bar{g}_a[v_\theta - E_K]}. \tag{21}$$

This is the value of a_h at which the minimum along the middle branch matches the minimum along the left branch of the quintic. Further observe that if $w_{\min} < w_{lk}$, then the trajectory of F lands on the middle branch. Assuming $\partial f/\partial w < 0$ beneath $\mathcal{C}_o$, a simple condition ensuring that the trajectory of F lands on the middle branch is

$$a_h(t_f) > a_h^*. \tag{22}$$

Thus, in order for F to land on the middle branch of $\mathcal{Q}_o$, thereby allowing the A current to delay the activity of F, two conditions must be met. First, the maximal conductance of the current ($\bar{g}_a$) needs to be large enough so that the right-hand side of (21) is less than 1. Second, F needs to spend enough time on the left branch for the A current to sufficiently recover from inactivation, so that Eq. (22) is satisfied.

3.4. *Determining t_a*

We now discuss how the A current and the inhibitory synapse interact to affect the activity of F. Although these two processes are independent, their interaction determines whether or not the F trajectory lands on the middle branch of the quintic and, if so, how long it stays there. Specifically, while F is in it silent state (between $t = 0$ and $t = t_f$) two processes evolve that determine t_a. First, g_s decays causing the w-value, denoted $w_{lk}(g_s(t_f))$, from which F leaves the silent state to be dependent on g_s (see Fig 6A). From Eq. (18) for the jump curve, we find that $w_{lk}(g_s(t_f))$ satisfies $g_s(t_f) + M w_{lk}(g_s(t_f)) = g_s^*$. Second, a_h grows, causing the middle branch of the v-nullcline to move down. As seen in Fig. 6A, if at the time $t = t_f$ (when F leaves its silent state), the minimum point of the middle branch is below $w = w_{lk}(g_s(t_f))$ (denoted by the horizontal dotted line), the F trajectory lands on the middle branch. As in the derivation of a_h^* in Eq. (21), the value of a_h (now referred to as $a_h^*(t_f, g_s)$) for which the minimum value of the left branch of the inhibited v-nullcline matches the minimum value of its middle branch can be calculated analytically. From Eq. (13), the middle branch of the v nullcline is given by

$$f(v_\theta, w) - \bar{g}_a a_h[v_\theta - E_K] - g_s[v_\theta - E_{\text{syn}}] = 0. \tag{23}$$

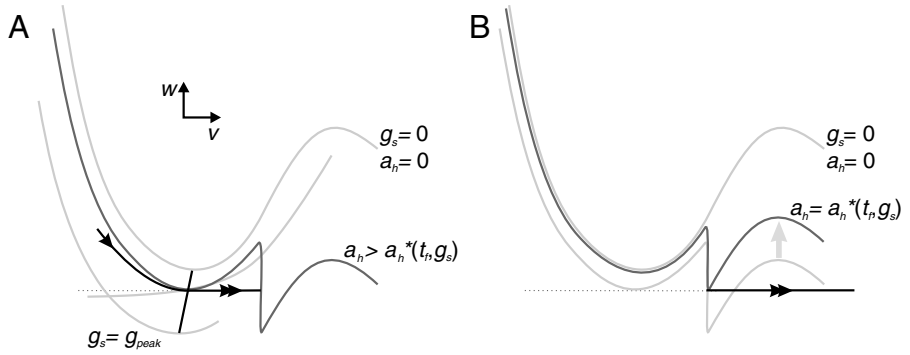

Figure 6. Dynamics before, during and after reaching the middle branch of the v-nullcline. (A) The trajectory of F lands on the middle branch only when the minimum w value along the middle branch is less than $w = w_{lk}(g_s(t_f))$, the minimum w value at which F leaves the silent state (dotted line). (B) The trajectory of F stays on the middle branch until the minimum w value along the middle branch equals $w = w_{lk}(g_s(t_f))$.

Thus, $a_h^*(t_f, g_s)$ satisfies

$$a_h^*(t_f, g_s) = \frac{f(v_\theta, w_{lk}(g_s(t_f))) - g_s(t_f)[v_\theta - E_{\text{syn}}]}{\bar{g}_a[v_\theta - E_K]}. \tag{24}$$

Note that when $g_s = 0$, then (24) reduces to (21). Thus, in general, the necessary condition for F to land on the middle branch of the quintic v-nullcline is that $a_h(t_f) > a_h^*(t_f, g_s)$. Substituting $a_h(t_f) = 1 - \exp(-t_f/\tau_{\text{lo}})$ and solving for t_f, we can derive an estimate on how large t_f needs to be in order for $t_a > 0$. Namely, if

$$t_f > \tau_{\text{lo}} \ln \frac{1}{1 - a_h^*(t_f, g_s)}, \tag{25}$$

then F will land on the middle branch of $\mathcal{Q}_o$ and $t_a > 0$. Otherwise, a_h is too small, causing the trajectory of F to jump directly to the right branch and thus $t_a = 0$. The inequality (25) implicitly gives information about the rate at which I_A deinactivates relative to the rate at which I_{syn} decays in the silent state. The right-hand side of (25) is most strongly affected by τ_{lo}, the time constant at which I_A grows when F is silent. The left-hand side is most strongly affected (for large g_{peak}) by τ_κ, the time constant controlling the decay of synaptic inhibition I_{syn} (as seen from Eq. (20)). Thus, if τ_{lo} is large, then inhibition must decay slowly to allow I_A to play a role in determining t_a. Indeed, if (25) is not satisfied, then $t_a = 0$.

When (25) is satisfied, we can derive an expression for t_a. On the middle branch, $a_h' = -a_h/\tau_{\text{med}}$. Thus

$$a_h(t) = [1 - e^{-t_f/\tau_{\text{lo}}}]e^{-(t-t_f)/\tau_{\text{med}}}. \tag{26}$$

On the middle branch $w = w_{lk}(g_s(t_f))$. During the time interval t_a, the conductances $\bar{g}_a a_h$ and g_s decay until the minimum on the middle branch of the quintic v-nullcline passes through the value $w = w_{lk}(g_s(t_f))$ (Fig. 6B). At this moment F leaves the middle branch and makes a fast excursion to the active state. Thus, the value of t_a can be calculated from Eq. (23) for the middle branch of the v-nullcline from the following equation

$$f(v_\theta, w_{lk}(g_s(t_f))) = \bar{g}_a a_h(t_f) e^{-t_a/\tau_{\text{med}}}[v_\theta - E_K] + g_s(t_f) e^{-t_a/\tau_\kappa}[v_\theta - E_{\text{syn}}]. \tag{27}$$

The right-hand side of (27) is a monotone decreasing function of t_a, while the left-hand side is independent of t_a. Thus (by the Implicit Function Theorem), for each value of t_f, there is a unique value of t_a which satisfies (27). This transcendental equation implicitly determines the value of t_a. If the inactivation of the A current is much slower than the decay of the inhibitory synapse ($\tau_{\text{med}} \gg \tau_\kappa$), Eq. (27) can be simplified by ignoring the second term on the right-hand side, and we obtain

$$t_a = \tau_{\text{med}} \ln \frac{\bar{g}_a[1 - e^{-t_f/\tau_{\text{lo}}}][v_\theta - E_K]}{f(v_\theta, w_{lk}(g_s(t_f)))}. \tag{28}$$

Equation (28) shows that if F spends a longer time (t_f) in its silent state (and if (25) is satisfied), the delay (t_a) produced by the A current becomes longer.

We have now calculated the times that the F neuron trajectory spends both on the left branch and on the middle branch of the v-nullcline. These results are summarized in Fig. 7 by showing a full cycle of the F neuron trajectory. In Fig. 7A, we show this trajectory in the $v - w$ phase plane with key transition points marked from the beginning of the O active state to the end of the cycle. Figure 7B shows the same transition points on the voltage trace of F. In this cycle, the slow equations determine the time intervals from 2 to 3 (t_f), from 4 to 5 (t_a) and from 6 to 7 ($P - t_f - t_a$). The transitions from 1 to 2, 3 to 4 and 7 to 1 are determined by the fast equations and in our analysis are instantaneous.

3.5. The Activity Phase as Function of Period

In this section we use the analytical formulas derived for t_f and t_a in the previous sections to calculate the activity phase ($\phi = (t_f + t_a)/P$) of F as function of P. We compare 4 cases, defined by the presence or absence of synaptic depression and of I_A in F. These results are shown in Fig. 9. In making this figure, the period is treated as a parameter and modified by changing T_{inact} while keeping T_{act} constant. The parameters and equations used to obtain these results are given in the Appendix.

Increasing T_{inact} allows for more recovery from depression and strengthens the synapse, i.e., g_{peak} in Eq. (12) becomes larger. A graph of Eq. (12) is shown in Fig. 8 by plotting g_{peak} versus P. For small values of P, g_{peak} is small, which corresponds to a weak synapse. In this case, T_{inact} is too small to allow the synapse to sufficiently recover from depression. Note that for T_{inact} large enough, the synapse maximally recovers from depression (g_{peak} asymptotically approaches $\bar{g}_{\text{syn}}$

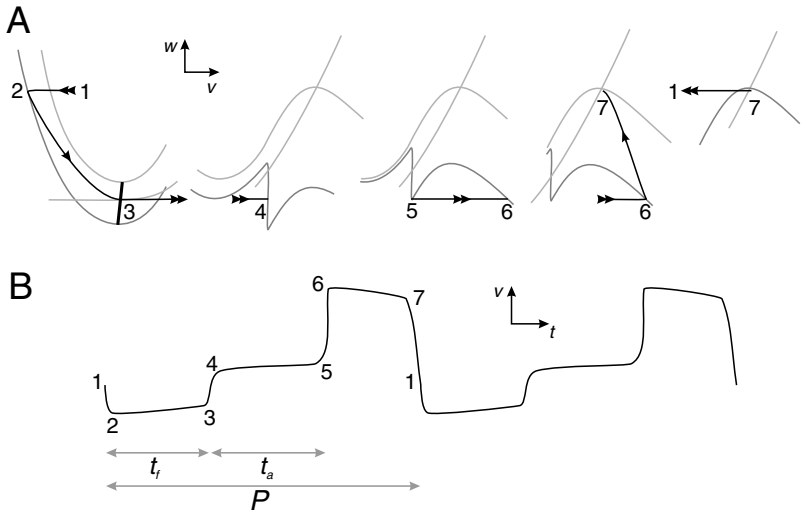

Figure 7. Nullclines and trajectory for a full cycle of F. (A) The various panels, from left to right, summarize the behavior of F's trajectory in the $v - w$ phase plane. The numbers in each picture corresponding to specific points as labeled in the lower panel. (B) The voltage trace of F in which relevant points from panel A are shown.

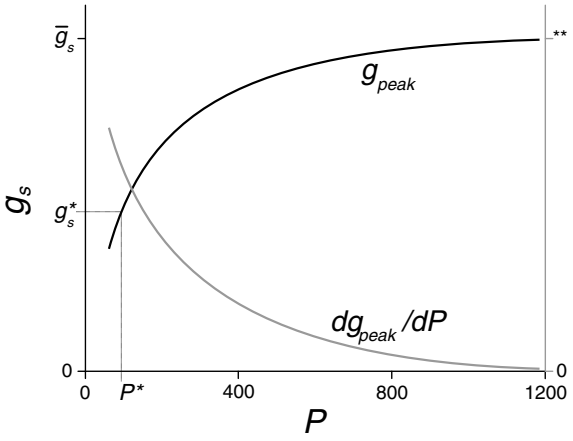

Figure 8. The peak synaptic conductance (g_{peak}, scale on left vertical axis) and its derivative (g'_{peak}, scale on right vertical axis) as a function of period. The plots were obtained by keeping T_{act} fixed and varying only T_{inact}. The value P^* is the period at which $g_{\text{peak}} = g_s^*$. The maximum value of g'_{peak}, denoted as $**$, is equal to $1/(1 - \exp(-T_{\text{act}}/\tau_\beta))$.

as $P \to \infty$). The derivative of g_{peak} with respect to P, although positive, exponentially decays to 0 as P increases (Fig. 8). We will use this fact later to calculate the phase of F activity.

Consider first the cases where the synapse from O to F is non-depressing. In these cases, t_f is fixed. If $I_A = 0$ or small, $t_a = 0$ and therefore the phase ϕ is a monotonic decreasing function of P (Fig. 9A). If I_A is sufficiently strong, $t_a > 0$ but is fixed and independent of P, because t_f is fixed. Thus the phase curve is again a monotonically decreasing function of P, albeit shifted up with respect to the case where I_A is small (Fig. 9B).

In the other two cases, the synapse from O to F is depressing, and therefore the strength of the synapse depends on the extent of depression and recovery from it. These, in turn, depend on the durations of the active and silent states (and thus period) of O. When I_A is non-existent or small, t_f is the only delay between the activity of O and F. In this case, with appropriate choice of parameters, the dependence of ϕ on P can be cubic (Fig. 9C), as explained below.

We can make use of the relationship between t_f and P (established by Eqs. (19) and (20)) to understand the dependence of phase ϕ on P when I_A is absent ($t_a = 0$ and $\phi = t_f/P$). When P is small g_{peak} is small, and Eq. (19) implies that t_f is constant. Thus, ϕ decreases with P. When P is large enough, Eq. (20) implies that t_f is an increasing function of P. This follows from the fact that g_{peak} is an increasing function of T_{inact} and therefore of P (Eq. (12) and Fig. 8). In this case, the dependence of ϕ on P is more complex. From Eq. (20) we see that

$$\phi = \frac{\tau_\kappa}{P} \ln \frac{g_{\text{peak}}}{g_s^*} + \frac{T_{\text{act}}}{P}.$$

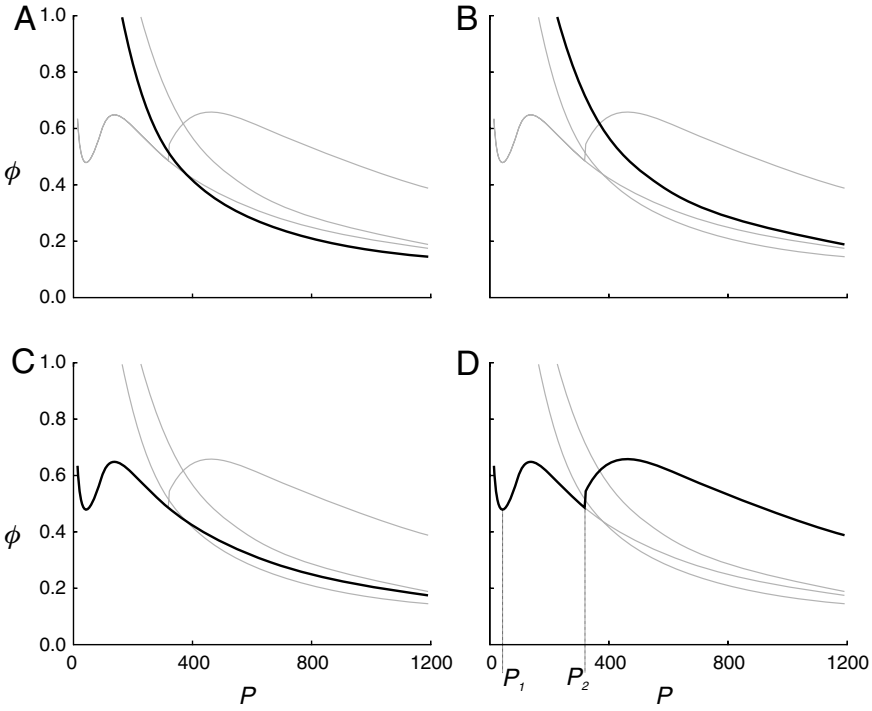

Figure 9. (A–D) Plots of the phase curves versus period in four conditions (each case is represented by a bold trace, other cases are plotted in gray). (A, B) The synapse is non-depressing, in the absence (A) and presence (B) of an A current in F. (C, D) The synapse is depressing, in the absence (C) and presence (D) of an A current in F. In D, the periods P_1 and P_2 indicate the local minima of the phase curve.

Whether ϕ is increasing or decreasing depends on the sign of the derivative $d\phi/dP$ given by

$$\frac{d\phi}{dP} = \frac{\tau_\kappa}{P}\left[\frac{dg_{\text{peak}}/dP}{g_{\text{peak}}} - \frac{1}{P}\ln\frac{g_{\text{peak}}}{g_s^*} - \frac{T_{\text{act}}}{P\tau_\kappa}\right].$$

Note that at the value of P ($=P^*$) for which $g_{\text{peak}} = g_s^*$ (Fig. 8), the expression $\frac{dg_{\text{peak}}/dP}{g_{\text{peak}}} - \frac{T_{\text{act}}}{P\tau_\kappa}$ is positive if either τ_κ is large enough or if T_{act} is small enough. The former condition means that the synapse decays slowly, while the latter means that the synapse has a very small amount of time to depress in each cycle. In these cases, $d\phi/dP > 0$ and thus, for P values close to P^*, ϕ increases with P.

Next consider the case where the cycle period is very large ($P \to \infty$). Then $g_{\text{peak}} \to \bar{g}_{\text{syn}}$ and $dg_{\text{peak}}/dP \to 0$ (Fig. 8). Since $dg_{\text{peak}}/dP \to 0$ exponentially fast (in particular, faster than $1/P$), $d\phi/dP < 0$ and thus ϕ decreases for large values of P. Thus, for the appropriate choice of parameters, as P increases from very small to very large values, ϕ is initially decreasing, then increasing and finally decreasing again (Fig. 9C).

Finally, when I_A is sufficiently strong, the delay between the onsets of activities in O and F is $t_f + t_a$, where t_a is a monotonic increasing function of t_f. This synergistic interaction give rise to the complex relationship shown in (Fig. 9D). In this case, the phase curve has two local minima and two local maxima and is qualitatively "quintic" shaped. The second set of local extrema is due solely to contribution of the A current. Let $P_1 < P_2$ denote the values of period at the two local minima. In this figure, we have chosen τ_{lo} large enough so that I_A does not become relevant until $P > P_2$. In this range of periods, t_a is primarily determined by the parameter τ_{med}, the inactivation time constant of the A current on the middle branch of $\mathcal{Q}_o$. This time constant is independent of both τ_L (the intrinsic time constant of F on the left branch) and τ_κ (the synaptic decay time constant) which, respectively, determined phase in the ranges $P < P_1$ and $P_1 < P < P_2$. Thus by choosing τ_{med} to be sufficiently large and τ_{lo} satisfying (25), a second set of local extrema was obtained.

The addition of I_A into the description of F provides the network with another way to determine phase.

There are now four important and independent time constants which determine phase, τ_L, τ_κ, τ_{lo} and τ_{med}. By choosing them appropriately, the phase curve can have 0 (monotonically decreasing), 2 (cubic shaped) or 4 (quintic shaped) local extrema. The analysis leading to Eqs. (18) and (27) shows which of these (and other) parameters control the locations of these extrema and the ϕ values at these points. For example, when τ_κ is small relative to τ_L, ϕ is determined solely by τ_L or τ_{med} and is monotonically decreasing. When τ_κ is large relative to τ_L, but τ_{med} is small or τ_{lo} is large relative to τ_κ, the phase curve is cubic. Finally, when τ_κ and τ_{med} are large relative to τ_L and τ_{lo} is not so large relative to τ_κ and satisfies (25), the phase curve is quintic shaped.

To elucidate the use of the analytical method in determining parameter values that produce a given phase in the model, we ran numerical simulations using Morris-Lecar type equations (Morris and Lecar, 1981) with an additional A current (see Appendix for equations). The equations were solved at three different periods of O and the resulting voltage traces of F are depicted (Fig. 10A). In the example shown, parameters of the model were chosen with the aid of the analytical solution such that the phase of activity of the follower neuron in each of these three periods was $\phi = 0.7$ (Fig. 10B). When $P = 150$, F becomes active after a time $t_f = 105$ which is mostly controlled by the intrinsic recovery variable of F. At $P = 300$, F becomes active after time $t_f = 209$. In this case, the synapse from O to F plays a larger role in setting the phase. Finally, when $P = 800$, F becomes active at $t_f + t_a = 402 + 158 = 560$ and the A-current, in conjunction with the synapse, now contributes to phase detemination. Note that at period values other than the ones shown, the value of phase (although not equal to 0.7) could still be determined by the analytical equations. These numerical simulations demonstrate the strength of our analytical results.

4. Discussion

Many behaviors are mediated by oscillatory networks and require proper phase relationships among the neurons involved. In olfactory processing, for example, different odors are encoded by patterns of phase of different neurons with respect to the field oscillation (Laurent et al., 1996). Hippocampal place cells use the phase of activity to encode for the location of the animal. The firing phase of the neuron with respect to the field theta rhythm advances as the animal moves through the neuron's place field (O'Keefe and Recce, 1993). Thus the activity phase of neurons need not be locked to the field oscillation but may change with a consistent pattern. In many central pattern generators (CPGs), the phase difference between different members of the CPG is often kept constant despite wide changes in frequency. For example, in chains of coupled oscillators, the phase difference between adjacent oscillators remains constant independent of frequency (Skinner and Mulloney, 1998). In the crustacean pyloric circuit, the tri-phasic pattern of activity is maintained despite large changes in frequency (Hooper, 1997a). This robustness emerges from the ability of pairs of neurons to maintain fixed phase when frequency changes (Hooper, 1997b).

A common question in all these systems is how the activity phase of neurons is controlled. We addressed this question in an inhibitory oscillator-follower

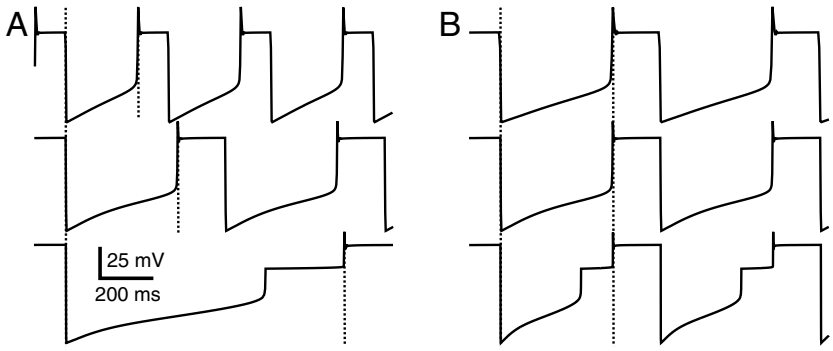

Figure 10. Numerically generated voltage traces of F at three different periods (150, 300 and 800, with $T_{\text{act}} = 20$). The dotted lines are the onsets of activity in the Oscillator and the Follower neurons in each of the three traces. The onset of O activity is aligned for all three traces. (A) The time to the onset of F activity increases as a function of period. (B) The same traces are shown with all time scales normalized to their respective period. In all three cases, F becomes active at the same phase $\phi = 0.7$ (the second dotted lines are aligned in all traces).

network. An inhibitory synapse can trigger the activation of a particular set of currents, which can subsequently advance or delay the activity of the follower. An important class of such currents are the transient potassium currents also known as A currents (Connor and Stevens, 1971). The A current refers to a family of inactivating potassium currents that have different genetic expressions. An important property of the A current is that it is usually inactivated at rest. Following hyperpolarization, the A current is deinactivated and, upon repolarization, can delay activity (Harris-Warrick et al., 1995; Hess and Manira, 2001; Hsiao and Chandler, 1995). Thus, the A current can set the timing of the first action potential a neuron fires following synaptic inhibition. Once the neuron is active, the A current inactivates and therefore its effects are transient.

In this work, we analyzed a simplified model network involving an inhibitory depressing synapse between an oscillator O and a follower F neuron that has an A current. In our model, we divided the latency between O and F into two distinct components, one incorporating the effects of synaptic inhibition of $F(t_f)$ and the other incorporating the effects of the A current (t_a). Using the derived mathematical expressions for t_f and t_a, we found that the A current delays the activity of F only when t_f is long enough, because in this case, t_a is an increasing function of t_f.

The mathematical expressions for t_a and t_f can be used to calculate the phase of F as a function of period. We have shown this relationship for the case where the period is changed by changing only the duration of the silent state of the oscillator. In this case, a non-depressing synapse produces a constant t_f and t_a, resulting in a monotonically decreasing phase curve. However, when the synapse is depressing, its strength changes with period. As a result, t_f and consequently t_a are dependent on period as well. With an appropriate choice of parameters the relationship between phase and period can be monotonic, cubic or quintic shaped. Thus, with a depressing synapse, the choice of model parameters allows different mechanisms to control the phase in different period ranges. For example, at small periods, when the synapse is weak, phase is determined by the intrinsic dynamics of F in its silent state (determined by τ_L). At intermediate periods, the synapse recovers from depression and phase is mostly determined by the decay time constant (τ_κ) of the synapse. At larger periods, the synapse is almost maximally recovered from depression. In this range, the A current dynamics (τ_{med}) determine phase. Note that the period-dependent contribution of the A current is a direct consequence of the period-dependent recovery of the inhibitory synapse from depression.

The important kinetic parameters that determine the effect of the A current on phase are the time constants of inactivation (τ_{med}) and deinactivation (τ_{lo}). The deinactivation time constant determines the magnitude of the A current upon activation. The inactivation time constant determines the delay between the release of the follower neuron from inhibition and its activity. In particular, if the A current deinactivates too slowly (relative to τ_κ; see Eq. (25) or inactivates too quickly, it would have little or no effect on the activity time of the neuron. The inactivation time constant (τ_{hi}) at higher membrane potentials, i.e., once the neuron is active has little significance in our analysis. However, in a spiking neuron the value of τ_{hi} could determine the spike rate once the neuron is active.

4.1. Implications of Simplifying Assumptions

To facilitate the derivation of an analytical expression for t_a, we made several simplifying assumptions on the dynamics of the A current. First, we assumed that the steady-state inactivation curve is a step function. The consequence of making this assumption is that the deinactivation of the A current is only dependent on time. However, experimental measurements of the dynamics of the A current show that the deinactivation of the A current can both be a function of voltage and time (Storm, 1990; Thompson, 1977). In contrast to our simplified case, if the deinactivation of the A current is voltage dependent, a_h will be affected by the level of hyperpolarization. In this case, a larger hyperpolarization would lead to a larger a_h, and thus a potentially larger contribution of the A current.

We also assumed that the activation curve of the A current is a step function. If it is voltage dependent, the middle branch of the v-nullcline is no longer vertical but would have negative slope and span a range of voltages. Hence, when the A current is activated, the voltage would gradually increase, as indeed is observed in experiments (Fig. 1). A voltage dependent activation curve would also have subtle effects on the phase curve. First, it would increase the minimum value of t_f necessary for t_a to be nonzero since a stronger A current would now be necessary for the minimum value along the middle branch to lie below the w value at which

the trajectory leaves the silent state. Secondly, it would shift the phase curve down since the inactivation variable a_h would not need to decay as much as in the voltage independent case. Thus t_a would be smaller.

The activation of the A current was taken to be instantaneous. Relaxing this condition would have the same qualitative effects as making the activation curve voltage dependent. We have also made the assumption that the A current inactivates on the middle branch at a faster rate than the evolution of the recovery variable w. In Hodgkin-Huxley type models, the recovery variable typically evolves very slowly at intermediate voltage values, consistent with our assumption. Removing this condition however, would shift the phase curve up as t_a would be larger in this case. Note that any other kind of simplifying assumption on the evolution of w can be used to do the same type of analysis on the middle branch. Finally, we have assumed that activation and inactivation of the A current occur between the left and right branches of the v-nullcline. If instead, we assume that these occur on the left branch, then the A current will have less time to deinactivate before it is activated. This would make the phase smaller at each period.

We also demonstrated that the dynamics of F could be described using Morris-Lecar type equations (see Fig. 10). The important aspects of the model neuron that are needed for the type of analysis we conducted are that the follower neuron have a high-voltage fixed point and a clearly identifiable recovery process.

Note that all these simplifying assumptions were made merely to make the calculations easier and explicit. Removing any or all of them does not qualitatively change the results that when the synapse is depressing, the phase can be determined by different parameters in different ranges of period.

4.2. *Different Types of Oscillators*

The derivation of the times t_f and t_a hold for any value of T_{inact} and T_{act}. Thus, the phase of the follower neuron can be calculated once T_{inact} and T_{act} are known. We used this fact to explore how phase changes as a function of period in the special case where period was changed by holding T_{act} fixed and changing T_{inact} (Fig. 9). In general, the phase versus period relationship can be obtained when the values of T_{inact} and T_{act} are known for any period. The qualitative relationship shown in (Fig. 9) will hold in any case where g_{peak} is an increasing function of period as in Fig. 8 (for example, when both T_{inact} and T_{act} increase but the duty cycle T_{act}/P remains constant).

Manor et al. (2003) studied how the phase changed as a function of period in three different cases: fixed T_{act}, fixed T_{inact} and fixed duty cycle. In the present work, we do not need to make this distinction since we have given equations that can be used to compute the phase-period relationship for any value of T_{inact} and T_{act}. In particular, the results numerically computed in Manor et al. (2003) could be analytically computed using equations involving t_f.

An important aspect that we have not explicitly considered is the issue of feedback from the follower to the oscillator. Although our analysis does not determine how feedback affects the oscillator, once the feedback network has reached steady state, the phase of the follower cell can still be determined using our mathematical expressions. It would be interesting to understand how different types of feedback affect T_{act} and T_{inact}, and consequently phase.

4.3. *Other Types of Currents*

In the current study we chose to focus on the effects of one type of intrinsic current in F. Other types of ionic currents could contribute to the activity phase of F as well. The present work provides a framework to study how other such currents may influence phase. We here mention a few examples.

A hyperpolarization activated inward (h) current may be activated by an inhibitory input and act to advance the activity of F. Since this current is activated at low voltages, its main effect is to decrease t_f. To derive a mathematical expression for t_f, the relationship between three variables, w, g_s and the activation of the h current, would need to be established on the left branch of the v-nullcline. The existence of an h current could also change the influence of the A current on phase since t_a depends on t_f.

It is intuitively clear that the h and A currents can have opposing effects on phase. However, this does not mean that these two effects cancel out, since it is possible that their primary influences occur in different ranges of periods. For example, if the time constant of activation of the h current is significantly larger than the time constant of inactivation of the A current, the h current will advance the phase of F at much larger periods than the A current delayed it. Thus the h current could be used to control the phase in a distinct range of periods, e.g. $P > P_2$ in Fig. 9.

Another example of an ionic current that, in conjunction with synaptic inhibition, can influence phase is a low-threshold calcium (T) current. As with the A current, T currents are transient and deinactivate upon hyperpolarization. In contrast to the A current, the inward T current advances the activity of F. In this regard the T current may act like the h current to reduce t_f. However, the T current activates in a different range of voltages, has faster kinetics than the h current and, most importantly, is a regenerative current. As such, the T current could have a significant effect in accelerating the activity of a biological neuron. In our reduced model, such a T current would have little effect by itself since the transition from the left to right branches of the v-nullcline is instantaneous. However, if F has an A current, the T current can decrease the delay t_a and thus advance the activity phase.

Appendix

We used MATLAB to numerically solve for t_f, t_a and ϕ. The equations we solved were

$$c_1 g_{\text{peak}} \exp(-(t_f - T_{\text{act}})/\tau_\kappa) + c_2 \exp(-t_f/\tau_L) = c_3. \tag{29}$$

$$g_{\text{peak}} = \bar{g}_{\text{syn}} \frac{1 - \exp(-T_{\text{inact}}/\tau_\alpha)}{1 - \exp(-T_{\text{inact}}/\tau_\alpha)\exp(-T_{\text{act}}/\tau_\beta)}. \tag{30}$$

The value of t_a was obtained from

$$r_1 \bar{g}_a (1 - \exp(-t_f/\tau_{\text{lo}}))\exp(-t_a/\tau_{\text{med}}) + r_2 g_{\text{peak}} \times \exp(-(t_f - T_{\text{act}})/\tau_\kappa)\exp(-t_a/\tau_\kappa) = r_3. \tag{31}$$

when $1 - e^{-t_f/\tau_{\text{lo}}} < c_4/\bar{g}_a$ and was 0 otherwise.

$$\phi = \frac{t_f + t_a}{T_{\text{inact}} + T_{\text{act}}} \tag{32}$$

We used the following set of parameters $T_{\text{act}} = 5$, $\tau_\kappa = 125$, $\tau_L = 15$, $\tau_\alpha = 400$, τ_β=5, $\tau_{\text{lo}} = 465$, $\tau_{\text{med}} = 1200$, $\bar{g}_{\text{syn}} = 4.0$, $\bar{g}_a = 3.5$, $c_1 = 4\exp(T_{\text{act}}/\tau_\kappa)$, $c_2 = 4.6$, $c_3 = 3$, $c_4 = 1.0$, $r_1 = 5.0$, $r_2 = 0.1$ and $r_3 = 5.0$. The term c_2 represents $M\hat{w}(g_{\min})$ and for simplicity we have assumed that $\hat{w}(g_{\min})$ is constant. The terms $c_3 = g_s^*$, $c_4 = a_h^*(t_f, g_s)$ where we have assumed the latter is constant. For cases where the synapse was nondepressing, (9A and B), we used $\bar{g}_a = 2.35$.

The voltage traces shown in Fig. 10 were obtained using XPP (Ermentrout, 2002). The oscillator was chosen to be a square wave oscillating between -50 and 0 with $T_{\text{act}} = 20$. We added an A-current to the Morris-Lecar equations (Morris and Lecar, 1981) for the follower cell. The equations for the follower cell are:

$$\begin{aligned} Cv' &= I_{\text{app}} - I_{\text{Ca}} - I_K - I_L - I_A - I_{\text{syn}} \\ w' &= [w_\infty(v) - w]/\tau_w(v) \\ a_h' &= [h_\infty(v) - a_h]/\tau_h(v) \\ d' &= [1 - d]H(v_{\text{thresh}} - v_O)/\tau_\alpha - d \\ &\quad \times H(v_O - v_{\text{thresh}})/\tau_\beta \\ s' &= -s_i H(v_{\text{thresh}} - v)/\tau_\kappa, \end{aligned} \tag{33}$$

where $I_{\text{Ca}} = 4m_\infty(v)[v - 120]$, $I_K = 8w[v + 84]$, $I_L = 2[v + 60]$, $I_A = \bar{g}_a a_{m_\infty} a_h[v + 84]$ and $I_{\text{syn}} = \bar{g}_{\text{syn}} s[v_O + 80]$. The voltage-dependent functions in the system are $m_\infty(v) = 0.5(1 + \tanh((v + 1.2)/18))$, $w_\infty(v) = 0.5(1 + \tanh((v - 15)/5))$, $\tau_w(v) = 40 - 30w_\infty(v)$, $h_\infty = 1/[1 + \exp([v + 7]/0.1)]$, $a_{m_\infty} = 1/[1 + \exp(-[v + 6]/0.5)]$, $\tau_h(v) = \tau_{\text{hi}} + [\tau_{\text{lo}} - \tau_{\text{hi}}]h_\infty(v) + [\tau_{\text{med}} - \tau_{\text{hi}}][H(v + 7) - H(v - 4)]$. The other parameter values are $C = 1$, $\bar{g}_a = 4$, $\bar{g}_{\text{syn}} = 4$, $\tau_\alpha = 600$, $\tau_\beta = 5$, $\tau_\kappa = 300$, $\tau_{\text{hi}} = 15$, $\tau_{\text{med}} = 700$, $\tau_{\text{lo}} = 500$, $I_{\text{app}} = 75$ and $v_{\text{thresh}} = -25$. The equations were integrated using the STIFF method. The variable s was reset to the value of d whenever v_O increased through v_{thresh} using the XPP GLOBAL command.

Acknowledgments

We thank Timothy Lewis for helpful discussions. This work was supported in part by NSF DMS-0315862 (AB), ISF 314/99-1 (YM), BSF 2001-039 (YM, FN) and NIMH 60605-01 (FN).

References

Ahissar E, Sosnik R, Haidarliu S (2000) Transformation from temporal to rate coding in a somatosensory thalamocortical pathway. Nature 406: 302–306.

Bartos M, Manor Y, Nadim F, Marder E, Nussbaum M (1999) Coordination of fast and slow rhythmic neuronal circuits. J. Neurosci. 19: 2247–2256.

Bose A, Manor Y, Nadim F (2001) Bistable oscillations arising from synaptic depression. SIAM J. Appl. Math. 62: 706–727.

Buchholtz F, Golowasch J, Epstein I, Marder E (1992) Mathematical model of an identified stomatogastric ganglion neuron. J. Neurophysiol. 67: 332–340.

Connor JA, Stevens CF (1971) Voltage clamp studies of a transient outward membrane current in gastropod neural somata. J. Physiol. (Lond.) 213: 21–30.

Connor JA, Walter D, McKowan R (1977) Neural repetitive firing: Modifications of the hodgkin-huxley axon suggested by experimental results from crustacean axons. Biophys. J. 18: 81–102.

DiCaprio R, Jordan G, Hampton T (1997) Maintenance of motor pattern phase relationships in the ventilatory system of the crab. J. Exp. Biol. 200: 963–974.

Ermentrout GB (2002) Simulating, Analyzing and Animating Dynamical Systems: A Gued to XPPAUT for Researchers and Students. SIAM, Philadelphia.

Harris-Warrick R, Coniglio L, Barazangi N, Guckenheimer J, Gueron S (1995) Dopamine modulation of transient potassium current evokes phase shifts in a central pattern generator network. J. Neurosci. 15: 342–358.

Hess D, Manira A (2001) Characterization of a high-voltage-activated ia current with a role in spike timing and locomotor pattern generation. Proc. Nat. Acad. Sci. 98(9): 5276–5281.

Hooper SL (1997a) Phase maintenance in the pyloric pattern of the lobster (*panulirus interruptus*) stomatogastric ganglion. J. Comput. Neurosci. 4: 191–205.

Hooper SL (1997b) The pyloric pattern of the lobster (*panulirus interruptus*) stomatogastric ganglion comprises two phase-maintaining subsets. J. Comput. Neurosci. 4: 207–219.

Hsiao C, Chandler S (1995) Characteristics of a fast transient outward current in guinea pig trigeminal motoneurons. Brain. Res. 695: 217–26.

Laurent G, Wehr M, Davidowitz H (1996) Temporal representations of odors in an olfactory network. J. Neurosci. 16: 3837–3847.

Manor Y, Bose A, Booth V, Nadim F (2003) The contribution of synaptic depression to phase maintenance in a model rhythmic network. J. Neurophysiol. 90, 3513–3528.

Marder E, Calabrese R (1996) Principles of rhythmic motor pattern generation. Physiol. Rev. 76, 687–717.

Mishchenko EF, Rozov NK (1980). Differential Equations with Small Parameters and Relaxation Oscillators. Plenum Press, New York.

Morris C, Lecar H (1981) Voltage oscillations in the barnicle giant muscle fiber. Biophys. J. 35: 193–213.

O'Keefe J, Recce ML (1993) Phase relationship between hippocampal place units and the EEG theta rhythm. Hippocampus 3: 317–330.

Pearson K, Iles J (1970) Discharge patterns of coxal levator and depressor motoneurons of the cockroach, *periplaneta americana*. J. Exp. Biol. 52: 139–165.

Rinzel J, Ermentrout G (1997) In: C. Koch and I. Segev, eds., Methods in Neuronal Modeling: From Synapses to Networks, MIT Press, Cambridge, MA, pp. 135–170.

Rush M, Rinzel J (1995) The potassium a-current, low firing rates and rebound excitation in hodgkin-huxley models. Bull. Math. Biol. 57: 899–929.

Skinner F, Mulloney B (1998) Intersegmental coordination of limb movements during locomotion: Mathematical models predict circuits that drive swimmeret beating. J. Neurosci. 18: 3831–3842.

Storm J (1990) Potassium currents in hippocampal pyramidal cells. Prog. Brain Res. 83: 161–187.

Thompson S (1977) Three pharmacologically distinct potassium channels in molluscan neurones. J. Physiol. 265: 465–488.